Journal of Applied Polymer Science

Polylactide and hybrid silicasol nanoparticle-based composites

Andrey Zhiltsov,[1,2] Oleg Gritsenko,[1*] Valentina Kazakova,[1] Olga Gorbatsevitch,[1] Natalia Bessonova,[3] Andrey Askadskii,[1] Olga Serenko,[1,2] Aziz Muzafarov[1,2]

[1]N.S. Enikolopov Institute of Synthetic Polymeric Materials, Russian Academy of Sciences, Moscow 117393, Russia
[2]A.N. Nesmeyanov Institute of Organoelement Compounds, Russian Academy of Sciences, Moscow 119991, Russia
[3]Karpov Institute of Physical Chemistry, Moscow 105064, Russia
Correspondence to: A. Muzafarov (E-mail: aziz@ispm.ru)

ABSTRACT: The effects of the chemical nature and size of the hybrid nanoparticle external layer on the structures and properties of polylactide composites are investigated. Polylactide is used as the matrix polymer, and molecular silicasol particles with γ-hydroxypropylic, (methoxyacetyl)oxy, and acetoxy surface groups serve as fillers. A preliminary assessment of the thermodynamic compatibility of polylactide with the surface groups of molecular silicasols is performed. The hydrophilic shells of the silicasols prevent their aggregation in the bulk of the nanocomposite. It shows variations in the chemical structure of the surface layer of the nanoparticles as well as their sizes and concentration make it possible to conduct a controlled change of the characteristics of the composites, particularly to eliminate one of the drawbacks of PLA, the low speed of its crystallization. © 2015 Wiley Periodicals, Inc. J. Appl. Polym. Sci. **2015**, *132*, 41894.

KEYWORDS: biodegradable; composites; extrusion; nanoparticles; nanowires and nanocrystals; structure-property relations

Received 25 July 2014; accepted 14 December 2014
DOI: 10.1002/app.41894

INTRODUCTION

Polylactide (PLA) and polylactide composites have attracted much research attention as transparent, biodegradable, and biocompatible materials with a vast scope of applications (from structural to packaging materials).[1,2] The PLA product line is constantly expanding; the number of companies that have launched trial consignments is increasing. This PLA product line expansion is also aided by the fact that PLA can be processed on standard equipment used for traditional heavy tonnage polymer production.[3,4]

Currently, different types of filling materials are used for controlled PLA material alterations to improve their processing properties and performance characteristics. Among these fillers, nanoparticles hold a specific niche because their introduction leads the polymer to obtain fundamentally new characteristics.[5–10] In a series of papers, the prospects for and the efficiency of using nanoparticle fillers of different natures and shapes (nanoclay, carbon nanotubes, silica, etc.) with PLA to decrease the gas transmission rate, increase the melt crystallization rate, and decrease the brittleness have been discussed.[4–11]

However, obtaining nanocomposites is accompanied by solving the complex problem of procuring a regular nanoparticle distribution within the polymer volume. High surface energy values at the nanoparticle–polymer interface promote the aggregation of the nanoparticles, which decreases the effectiveness of filling.[12,13] The use of surfactants or anti-adhesive precoatings can be used to induce conventional filler disaggregation processes in the polymer matrix.[10–16] The use of core-shell hybrid nanoparticles is one of up-to-date methods used to prevent nanoparticle aggregation.[17–19] If the shell has good polymer affinity, it can prevent aggregation of the filling material. Using this technique, it is possible to form nanocomposites using the shelf equipment of thermoplastic processing (mixing tanks and extruders) without any supplementary technological stages such as mixing or homogenization.

It has been established that the compatibility of the mixture components is defined mostly by their chemical structure.[20] In the current work, the degree of impact of the filler size and the surface groups chemical nature on the glass transition temperature as well as the cold crystallization and melting parameters is discussed.

*Deceased.

Additional Supporting Information may be found in the online version of this article.

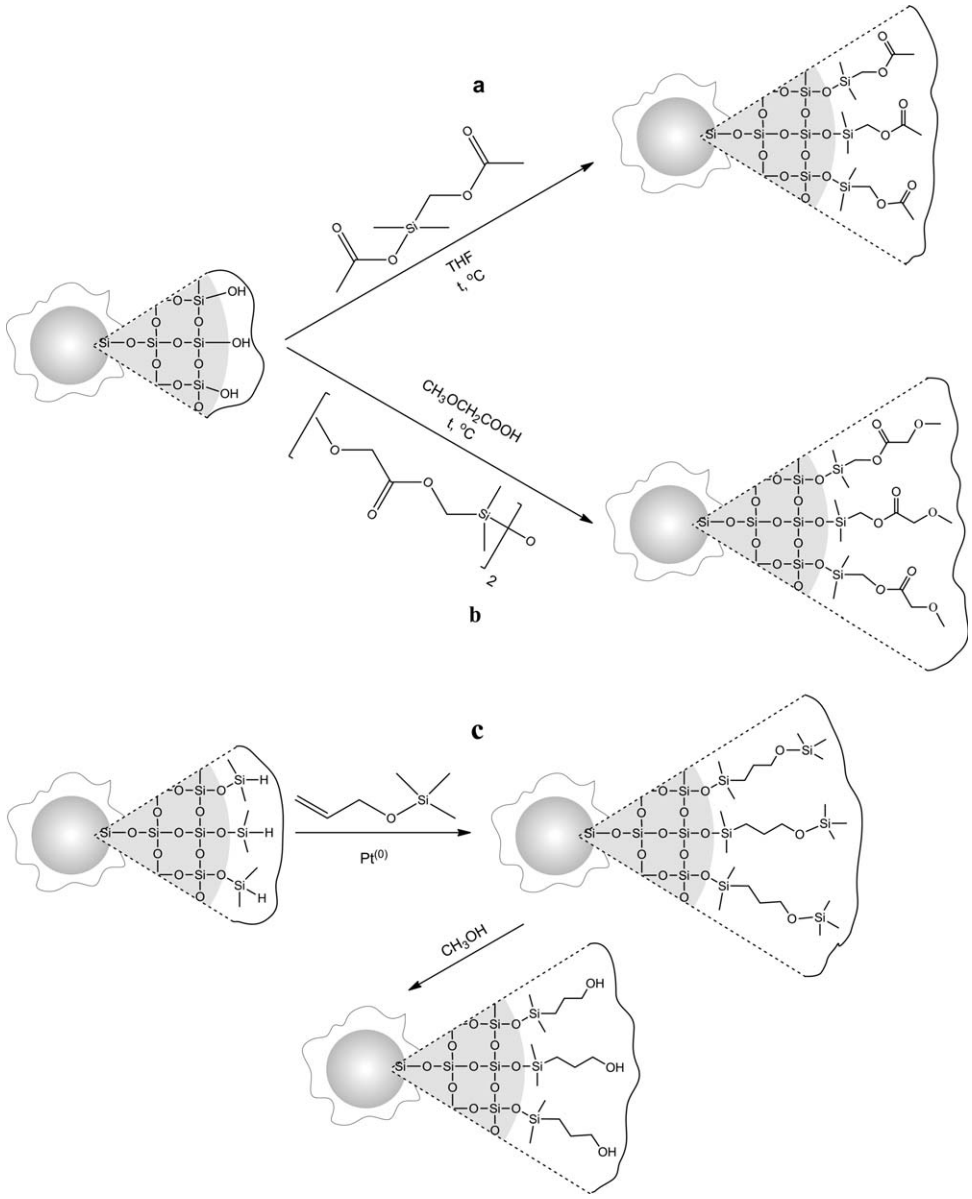

Figure 1. Synthesis of hybrid molecular particles with (methoxyacetyl)oxy (a), acetoxy (b), and γ-hydroxypropylic surface groups (c).

EXPERIMENTAL

PLA 4032D (NatureWorks LLC) with a $M_w = 1.7 \times 10^5$ g mol^{-1} and a $M_w/M_n = 1.74$ was used as the matrix polymer. Molecular silicasol particles with γ-hydroxypropylic, (methoxyacetyl)oxy, and acetoxy surface groups served as fillers. Synthetic strategies and particles surface modifications have been previously described,[21] and the synthetic schemes are shown in Figure 1. The experimental procedures are described in Supporting Information; infrared (IR) and proton nuclear magnetic resonance (^{1}HNMR) spectra of the particles are shown in Supporting Information Figures S1–S5. Particles with radii of $R = 0.7$ or 1.7 nm (γ-hydroxypropylic and (methoxyacetyl)oxy derivatives) and $R = 0.7$ or 1.5 nm (acetoxy derivatives) were obtained by blocking the growth of the core at different stages. The particle size distribution (Figure 2) was determined by the universal calibration method[22] using gel permeation chromatography (GPC) on a chromatographic system comprised of an Akvilon Staier high-pressure pump (Russia), a Smartline RI 2300 refractometric detector (KNAUER, Germany), and a Jetstream 2 Plus (KNAUER, Germany) column thermostat. The thermostat temperature was 40°C (± 0.1°C), and the eluent used was tetrahydrofuran (THF) at a flow rate of 1.0 mL min^{-1}. A column of 300 × 7.8 mm was filled with Phenogel sorbent (Phenomenex) with a particle size of 5 μm and a pore size of 10^3 Å (certified separation range up to 75000 Da). The data collection and calculations were performed using UniChrom 4.7 software (Belarus).

Nanoparticle polymer blends were obtained in a DACA Instruments (USA) double-screw bypass extruder at a temperature of 190°C and a rotor rotation speed of 500 min^{-1} over a 5-min period. Granulated polymer was predessicated at 50°C for 8 h.

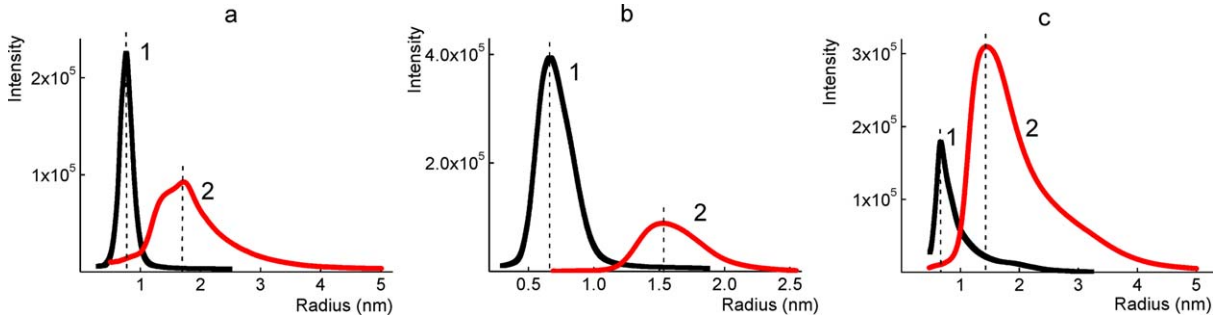

Figure 2. Size distributions of "small" (1) and "large" (2) silicasol particles with (methoxyacetyl)oxy (a), acetoxy (b), and γ-hydroxypropylic surface groups (c) (according to GPC data). [Color figure can be viewed in the online issue, which is available at wileyonlinelibrary.com.]

Calorimetric analyses were carried out on a DTAS-1300 (Russia) thermoanalyser from 20 to 190°C with a heating rate of 16°C min^{-1}. A minimum of five samples were tested. The glass transition temperature (T_g), crystallization temperature (T_{cc}), and melting point (T_m) were measured after repeated sample heating in the calorimetric cell. The beginning temperature of the polymer melt crystallization (T_{cm}) was measured on a METTLER STAR SW 8.00 (Switzerland) thermoanalyser at a cooling rate of 10°C/min^{-1}. The samples were melted beforehand in the calorimetric cell at 200°C.

The temperature corresponding to the specific heat inflection point at the devitrification stage of the sample was taken as a basis for the glass transition temperature. The temperatures of crystallization and melting were established as the temperatures at the beginning of these processes that corresponded to the thermograph baseline excursion points (Figure 3).

The compatibility of PLA with silicasol particles with modified surfaces was calculated by the method described elsewhere[23,24] using Kaskad software (Russia). Known equations were used for assessing the following characteristics:

solubility parameter δ (J cm^{-3})$^{0.5}$

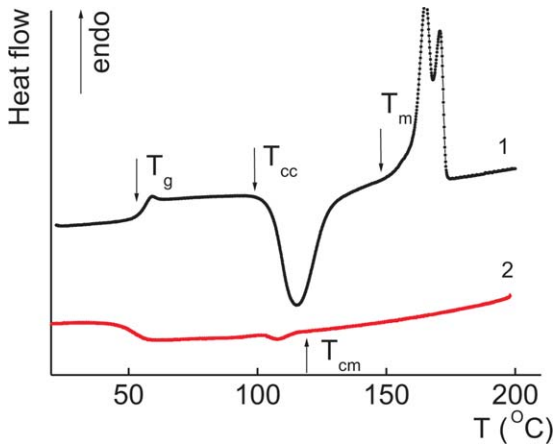

Figure 3. Thermograms of PLA melting (1) and crystallization (2). The following measured temperatures are indicated by arrows: glass transition T_g, cold crystallization T_{cc}, melting T_m, and melt crystallization T_{cm}. [Color figure can be viewed in the online issue, which is available at wileyonlinelibrary.com.]

$$\delta^2 = \frac{\sum_i \Delta E_i^*}{N_A\left(\sum_i \Delta V_i\right)} \quad (1)$$

surface tensions of the "solvent" γ_s and polymer γ_p (mN m^{-1})

$$\gamma_s = A_j \frac{\sum_i \Delta E_i^*}{\left(\sum_i \Delta V_i\right)^{2/3}} \quad (2)$$

$$\gamma_p = C_j \frac{\sum_i \Delta E_i^*}{\left(\sum_i \Delta V_i\right)^{2/3} m^{1/3}} \quad (3)$$

and molar volume V (cm^3 mol^{-1})

$$V = \frac{N_A \sum_i \Delta V_i}{k_{cp}} \quad (4)$$

where ΔE_i^* is the contribution of each atom and type of intermolecular interaction into the cohesion energy of a low-molecular-weight compound or polymer; $\left(\sum_i \Delta V_i\right)$ is the Van der Waals volume of a liquid molecule or polymer repeating unit; N_A is Avogadro's constant; A_j is a factor associated with coefficients of the molecular packing of liquid molecules in bulk and on the surface; C_j is the parameter associated with the molecular packing coefficients of polymers and is dependent on the polymer type; and m is the number of atoms in the polymer repeating unit.

RESULTS AND DISCUSSION

To determine the possibility of preparing a nanocomposite where the filler will be dispersed down to a nanosized scale, we assessed the thermodynamic compatibility of modified silicasol particles with PLA. Silicasol terminal groups were considered as the polymer "solvent". In Table I, the calculated values of the solubility parameters, surface tensions and polymer and "solvent" molar volumes necessary for the estimation of the thermodynamic compatibility between components are shown.

The thermodynamic compatibility of polymers has been studied in a great number of papers. In particular, the calorimetric investigations of blends of poly(vinyl acetate), poly(vinyl butyrate), poly(methyl acrylate), and poly(propyl acrylate) were made[25]. It was shown that the heat of mixing depends on the chemical structure of the blend components. As to the

Table I. Calculated Parameters Necessary for the Estimation of the Thermodynamic Compatibility

		Silicasol surface group type		
Parameter	PLA	γ-Hydroxypropylic	(Methoxyacetyl)oxy	Acetoxy
Solubility parameter, δ [(J cm^{-3})$^{0.5}$]	20.5	20.85	18.4	19.78
Surface tension, γ (mN m^{-1})	36.1	25.9	26.6	27.52
Molar volume, V (cm^3 mol^{-1})	55.1	134.9	103.0	73.6

prediction of compatibility, the interaction parameter $\chi_{1,2}$ of Flory–Prigogine–Patterson modified by Delmas was calculated. In a series of papers,[26–28] the morphology and the thermal, mechanical, and rheologic properties of blends based on ethylene and 1-octen copolymers were analyzed. The blends prepared by two different cooling process (fast cooling and slow cooling) were not homogenous regardless of the density, melt index, and comonomer content. The use of Ziegler–Natta catalysts in the synthesis of these copolymers exhibited a bigger spherulitic diameter and a larger ring space compared to those of metallocene prepared by a cooling process.

Consideration of the thermodynamics of polymer mixtures is useful for the analysis of their compatibility and properties. However, in this study, the compatibility of two polymers is not considered. The subject of the study is the description of polymer "solubility" in low-molecular-weight liquids of molecules grafted on the surface of the nanoparticles. Therefore, we use the criterion of polymer solubility.

The physical assumptions used in determination of solubility conditions have been previously described.[23,24] When a polymer sample is immersed into a solvent, the globules on the sample surface are detached first. Simultaneously, the solid (globule)–liquid interphase is formed. The formation of the unit of this surface includes work W_A determined by the process of adhesive wetting:

$$W_A = \gamma_{s-p} - (\gamma_p + \gamma_s) \tag{5}$$

where γ_p and γ_s are surface tensions of polymer and solvent, respectively; $\gamma_{s\text{-}p}$ is the interfacial tension. In eq. (5), W_A represents the work of adhesion, that is, the work required for separation of the surfaces (e.g., recovery of the initial state). The presence of this work leads to the occurrence of forces that affect the globule depending on the value and sign of globule curvature. These forces result in detachment of the globule from the polymer sample. When this detachment happens and the globule goes into the solvent, a new surface of another globule, which was previously closed, is formed. The new globule is also wetted by the solvent, and the same forces appear. When this globule is detached, the process is repeated.

If the surface of the polymeric body is constructed of globules, they are subject to the following forces: (1) the compression force, which is proportional to the positive curvature of the globule; (2) the force of wedging in the case of a negative curvature at the junction of the globule to the surface; (3) the strength of intermolecular interactions between solvent and polymer. All of these forces have been discussed in detail.[23,24] If the forces 2 and 3 are greater than force 1, the globule leaves the surface. As a result, the components of a mixture are known to be thermodynamically compatible if the following inequality takes place:[23,24]

$$\frac{\delta_p^2}{\delta_s^2}\left(\frac{M}{M_0}\right)^{1/6} < \left[2\rho\Phi\left(\Phi - \sqrt{\Phi^2 + \frac{\gamma_p}{\gamma_s} - 2\Phi\left(\frac{\gamma_p}{\gamma_s}\right)^{1/2}}\right)\right] \tag{6}$$

where

$$\Phi = \frac{4\left(V_s V_p\right)^{1/3}}{\left(V_s^{1/3} + V_p^{1/3}\right)^2}$$

Herein, $M_0 = 200{,}000$ is the molecular weight of the polymer at polymerization degree N_0, which equals 2770 for polylactide; M is the molecular weight of the polymer; and δ_p, V_p, γ_p, δ_s, V_s, and γ_s are the solubility parameters, molar volumes, and surface tensions of the polymer and the solvent, respectively. Hereinafter, we in symbol:

$$A = \frac{\delta_p^2}{\delta_s^2}\left(\frac{M}{M_0}\right)^{1/6}$$
$$B = \left[2\rho\Phi\left(\Phi - \sqrt{\Phi^2 + \frac{\gamma_p}{\gamma_s} - 2\Phi\left(\frac{\gamma_p}{\gamma_s}\right)^{1/2}}\right)\right] \tag{7}$$

Therefore, inequality (6) can be written as $A < B$. In Table II, there are parameter values for the systems examined on the assumption that the degree of PLA orientation equals zero.

Table II. A and B Parameter Values (PLA-Modified Silicasol System)

Molecular weight of PLA (Da)	A	B	Compatibility
PLA–acetoxy surface groups			
3.1×10^5	1.155	1.163	+
3.2×10^5	1.162	1.163	+
3.3×10^5	1.168	1.163	–
PLA–γ-hydroxypropylic surface groups			
3.0×10^5	1.035	1.041	+
3.1×10^5	1.040	1.041	+
3.2×10^5	1.046	1.041	–
PLA–(methoxyacetyl)oxy surface groups			
0.9×10^5	1.087	1.104	+
1×10^5	1.106	1.104	–

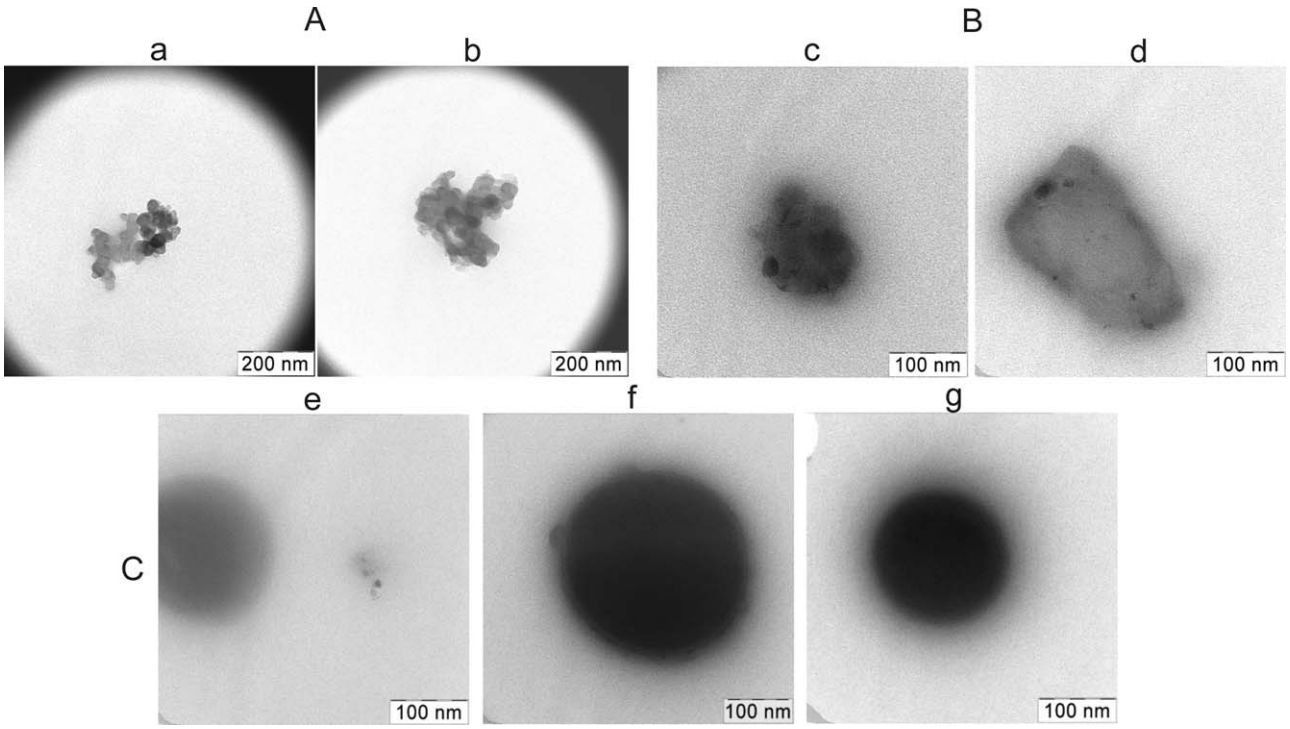

Figure 4. Types of aggregates for silicasol particles in PLA: random aggregates of individual particles (A), friable (nonclosely packed) aggregates of irregular shapes (B), and solid spherical formations with diffuse interfaces (C). Concentration of particles: with acetoxy surface groups 5 (a) and 1 wt % (d); with (methoxyacetyl)oxy groups 5 (b,g) and 2 wt % (e,f); and with γ-hydroxypropylic groups 2 wt % (c). Particle sizes: 1.4 (a–e,f) and 3.4 nm (e).

From the data acquired from the PLA system, for acetoxy surface groups an adequate inequality (6) is accomplished up to a matrix polymer molecular weight of 3.2×10^5 g mol^{-1}. In the case of PLA and γ-hydroxypropylic surface groups, compatibility is observed as long as the PLA molecular weight does not exceed 3.1×10^5 g mol^{-1}. The PLA molecular weights that are compatible with (methoxyacetyl)oxy surface groups (less than 0.9×10^5 g. mol^{-1}) are significantly smaller than for the other surface groups. Note that the M_w of the matrix polymer used in the work is 1.7×10^5g mol^{-1}.

In terms of the acquired estimated data, we can conclude that the efficiency of the nanoparticle surface organic layer, that performs the function of making the PLA and filler compatible, is high and virtually the same for acetoxy and γ-hydroxypropylic surface groups, and it is less in case of (methoxyacetyl)oxy groups grafted to the surfaces of silicasol particles. In the latter case, the composition can be characterized as a system with components of limited compatibility.

In cases of limited compatibility of the nanoparticle surface groups with the polymer, the probability of obtaining a material where the filler is going to remain nanosized and not aggregate is low. However, the structure of the mixture of incompatible compounds is determined not only in accordance with the thermodynamic compatibility of its components but also by the mixing conditions as well. As is known, the use of a double-screw extruder can allow the dispersion of unmodified filler into the polymer on a nanoscale level to be achieved provided that the total particle loading is not above 2–5 vol %.[29]

According to the results of the microscopic analysis, both individual inclusions and a small amount of cluster agglomerates are observed in composites based on PLA and surface-modified silicasol particles. The range of sizes of these formations is rather wide. However, it is estimated that the maximum dimension of the agglomerates increases in size with the deterioration of the surface group compatibility with the matrix polymer. Therefore, in the case of the introduction of particles with γ-hydroxypropylic surface groups, the maximum dimension of the agglomerates does not exceed 230 nm, with acetoxy groups, it is no more than 300 nm, and with (methoxyacetyl)oxy groups, it is no more than 500 nm. It is worth noting that the maximum diameters of the agglomerates are dependent, to a great extent, on the compatibility of PLA and the surface groups and to a smaller extent on the size and concentration of the particles.

Consequently, if compositions are obtained by the extrusion mixing method, the use of hybrid particles, the organic shell of which is highly compatible with the matrix polymer, really prevents the formation of agglomerates with diameters that go beyond the scope of the nanometer scale. The size of the small amount of large filler agglomeration does not exceed 300 nm.

Figure 4 shows an example of the most typical nanoparticle agglomerates in the composites. The first type is random agglomerates of individual particles [Figure 4(A)]; the second type is friable (nonclosely packed) agglomerates with irregular shapes [Figure 4(B)]; and the third type is solid spherical formations with diffuse interfaces, which points to the undercoat diffuse layer formation between the sphere of the particle "agglomeration" and the matrix [Figure 4(C)].

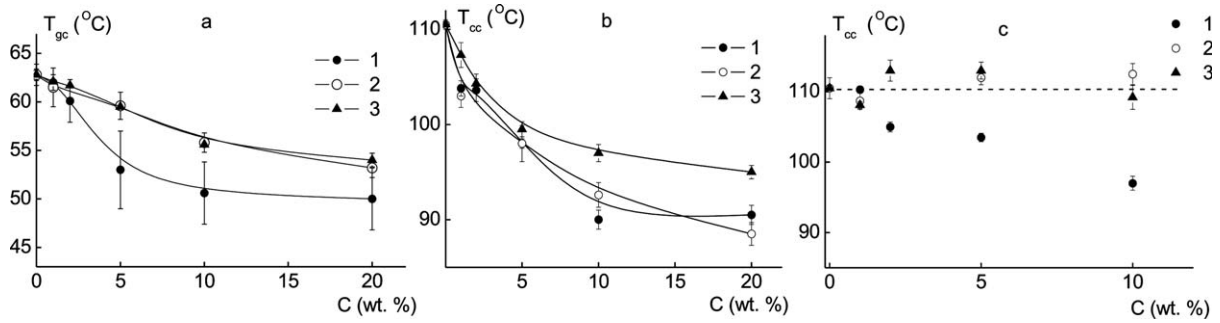

Figure 5. Glass transition temperatures (a) and cold crystallization temperatures (b,c) of composites based on PLA and nanosized silicasol particles with (methoxyacetyl)oxy (1), acetoxy (2), and γ-hydroxypropylic (3) surface groups. Silicasol particle radii: 0.7 (a,b) and 1.5 or 1.7 nm (c). The cold crystallization temperature of unfilled PLA is indicated by a dashed line.

Observing the formation of the above-mentioned particle agglomerates, we can draw a conclusion that the surface tension values of the outer layers of the particles (Table I) are not low enough for the spontaneous dispersion of nanosized filler particles in the PLA melt. As a result, in the case of mixing the filler with the polymer, two contrary processes of dispersion and coalescence involving not only individual particles but their agglomerates as well take place. It is necessary to note that over the entire range of filler concentrations studied the composites remain transparent notwithstanding their particle sizes and the chemical nature of their organic surface layers.

Upon the application of heat to the tested systems, the following repeated phase transitions are sequentially observed: glass transition, crystallization and melting (Figure 3). The crystallization, which takes place after the polymer glass transition, is commonly referred to as cold. Compositions obtained by extrusion mixing are amorphous because the heats of cold crystallization and melting are equal. The lack of a crystalline phase within the material is also proven by the results of X-ray diffraction analysis (XRD). The dependence of the composite glass transition temperature (T_{gc}) on the filler concentration (C_f) is shown in Figure 5(a). At the introduction of particles with relatively small radii (0.7 nm), the glass transition temperature drops monotonously, and this is indirect proof of the absence of microscaled aggregation in this system.[13] In the case of an increase in the amount of filler content, the temperature rate drop is defined by the thermodynamic compatibility level of the nanoparticle organic surface layer with the matrix polymer. In cases where there is good compatibility between the surface groups and PLA, the decrease in the composite glass transition rate is less than in cases where polymer hybrid particles are introduced that have limited compatibility with the matrix polymer at the surface level. Therefore, the T_{gc} experimental data for composites containing particles with acetoxy and γ-hydroxypropylic surface groups (high compatibility with PLA) demonstrate a similar type of dependence and lie over the graph that demonstrates the T_{gc} values for systems containing particles with (methoxyacetyl)oxy surface groups (limited compatibility with PLA).

The degree of impact of the filler surface groups on the glass transition temperature is determined by the size of the particles. In the case of PLA filled by particles with radii of 1.5 or 1.7 nm, regardless of the compatibility level of their surface layer with the polymer matrix, the glass transition temperatures of the mixtures vary only slightly when compared with the initial polymer (Table III). The differences in the data summarized in the table do not exceed 2%.

It is assumed in the paper[30] that the alteration of the glass transition of the composites with hybrid nanosized particles is mainly caused by the following conditions:

i. an increase in the number of degrees of freedom and the system entropy because of the presence of the organic layer on the surfaces of the hybrid nanoparticles, which contributes to a drop in the glass transition temperature;
ii. a depression in the disordering entropy of the system and the number of macromolecular configuration states with the present nanoparticles, which results in the composition glass transition temperature rising.

The competition of these two key factors ultimately determines the rise or depression of the glass transition temperatures of the materials with an increase in the hybrid nanoparticle content.

In the case of systems with nanoparticles with radii of 0.7 nm, their glass transition temperatures decrease with an increase in the concentration of the nanoparticles. Hence, in this case, the input of the first factor prevails over the second one. The glass transition temperatures of composites with nanoparticles with radii of 1.5 or 1.7 nm essentially do not depend on the

Table III. Glass Transition Temperatures of Composites with "Large" Surface-Modified Silicasol Particles

Particle concentration (wt %)	Surface group types and radii of silicasol particles		
	(Methoxyacetyl) oxy ($R = 1.7$ nm)	Acetoxy ($R = 1.5$ nm)	γ-Hydroxypropylic ($R = 1.7$ nm)
0	62.8 ± 0.6	62.8 ± 0.6	62.8 ± 0.6
1	62.9 ± 0.5	62.3 ± 0.5	64.5 ± 0.6
2	63.4 ± 0.6	64.2 ± 0.7	64.5 ± 0.6
5	62.3 ± 0.5	62.9 ± 0.5	63.4 ± 0.8
10	61.0 ± 0.4	60.5 ± 0.5	62.3 ± 0.8

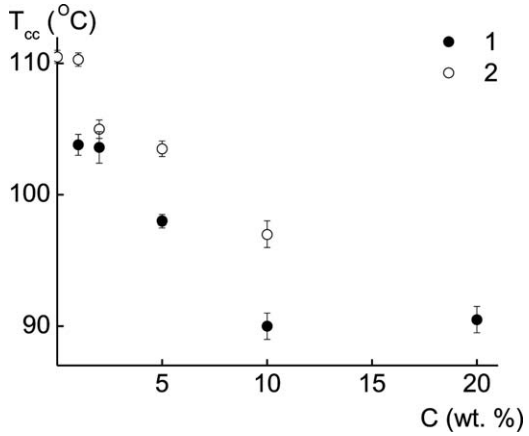

Figure 6. Cold crystallization temperatures of composites based on PLA and molecular silicasol with (methoxyacetyl)oxy surface groups. Particle radii: 0.7 (1) and 1.7 nm (2).

nanoparticle concentration. In this case, the two above-mentioned factors balance each other out.[30]

Figure 5(b) shows data on composites containing nanoparticles with radii of 0.7 nm by plotting the cold crystallization temperature (T_{cc}) versus the particle content. The T_{cc} values steadily decrease throughout the entire interval of nanoparticle contents studied. However, the phenomenon of the compatibility level of the surface layer of the particles with the polymer is not observed in an explicit form, as is the case for the concentration-dependent glass transition temperature variation of the systems examined. As for PLA with silicasol particles with (methoxyacetyl)oxy and acetoxy surface groups, their cold crystallization concentration temperature dependencies are close to but are lower than those for composites containing particles with γ-hydroxypropylic surface groups.

It is possible that the T_{cc} values of mixtures with hybrid particles with radii of 0.7 nm are dependent to a greater degree on the nature of the silicasol surface layer rather than on its compatibility level with PLA. The (methoxyacetyl)oxy and acetoxy derivatives contain ester units (CH_2–O–C(O)–) and differ only in the presence of an additional methoxide group. Apparently, the presence of a single-type polar group in the chemical structure of the external layer of the particles influences the matrix cold crystallization conditions to a greater extent than the thermodynamic compatibility level of the organic layer. This fact predetermines the T_{cc} data similarity for compositions with particles having (methoxyacetyl)oxy and acetoxy surface groups.

In cases of PLA fillings with larger particles with radii of 1.5 and 1.7 nm and highly polymer compatible organic layers (acetoxy and γ-hydroxypropylic groups), the T_{cc} values are practically unchanged and only a little different from the initial PLA T_{cc}. However, the introduction of particles with grafted (methoxyacetyl)oxy surface groups (limited PLA compatibility) leads to decreases in the matrix polymer cold crystallization temperatures [Figure 5(c)].

It can be assumed that the cold crystallization temperatures of composites with hybrid particles are determined by a number of factors, such as particle concentration, their size, their organic shell chemical structure and its compatibility with a matrix polymer and, possibly, the number and type of agglomerates formed. Each of these factors determines the significance of the other ones. For example, the degree of impact of the PLA surface layer compatibility on the T_{cc} depends on the particle size and content. On the other hand, the influence of the particle concentration on the T_{cc} is determined by both the particle size and the level of the particle surface layer compatibility. The last of the above-mentioned factors is rather well illustrated by the following measured data: T_{cc} values decrease with the growth of the silicasol content if the surface layer is compatible with the matrix polymer (acetoxy and γ-hydroxypropylic groups) and if the radius of the inclusions is 0.7 nm. The T_{cc} values remain stable if the radius of inclusions is 1.5–1.7 nm. Figure 6 shows the curves of the T_{cc} dependence on the C_f for PLA mixtures with different sizes of silicasol with (methoxyacetyl)oxy surface groups (limited PLA compatibility). The T_{cc} values of the composites decrease with an increase in the filler content, but in composites with larger particles, the cold crystallization temperatures are higher than in those composites with smaller particles.

The melting temperatures (T_m) of the composites examined vary only slightly, and the variation in the remainder of the values obtained for the initial PLA and the mixtures do not exceed 2°C (Table IV). Hence, the T_m is the least sensitive characteristic of the material in relation to its content, particle size and type of grafted surface groups.

Table IV. Melting Temperatures of Composites Based on PLA- and Surface-Modified Silicasol Particles

	Surface group type					
Particle concentration (wt %)	(Methoxyacetyl)oxy		γ-Hydroxypropylic		Acetoxy	
	Particle radius (nm)		γ-Hydroxypropylic		Acetoxy	
	0.7	1.7	0.7	1.7	0.7	1.5
0	164	164	164	164	164	164
1	165	163	162	166	166	163
2	162	165	166	165	-	-
5	165	165	166	165	166	167
10	163	163	164	164	163	164

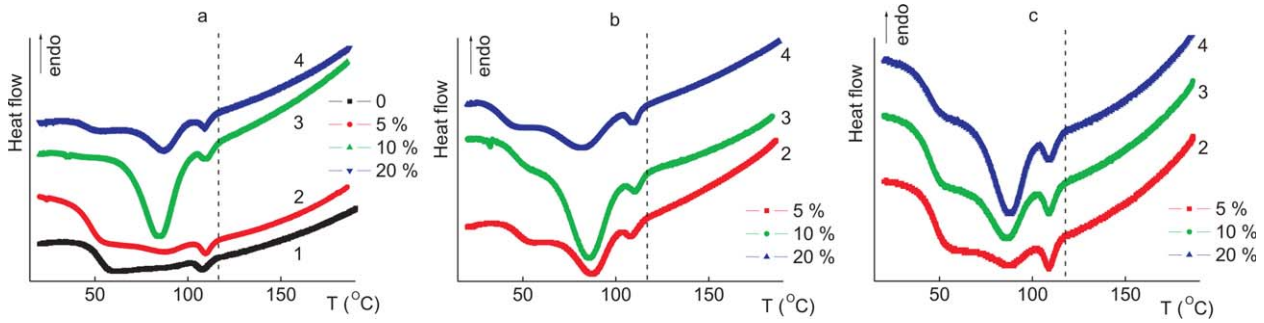

Figure 7. Crystallization thermograms of composites based on PLA and silicasol particles with (methoxyacetyl)oxy (a), acetoxy (b), and γ-hydroxypropylic (c) surface groups. Filler concentration: 0 (1), 5 (2), 10 (3), and 20 wt % (4). The composite crystallization starting point is marked by a dashed line. [Color figure can be viewed in the online issue, which is available at wileyonlinelibrary.com.]

Table V. Specific Heats of the Matrix Polymer Composite Melt Crystallization ($J\ g^{-1}$)

Particle concentration (wt %)	(Methoxyacetyl)oxy		Surface group type Acetoxy		γ-Hydroxypropylic	
	Particle radius (nm)					
	0.7	1.7	0.7	1.5	0.7	1.7
0	1.0					
1				2.6		
2	1.0	1.3			2.2	1.0
5	2.4	1.5	12.6	1.6	2.4	1.2
10	30	3.0	20.0	1.1	6.6	2.2
20	12.5		8.4		11.6	

Figure 7 shows a typical crystallization thermogram of the compositions examined. Notwithstanding of their size, the nature of surface groups and matrix compatibility level, the silicasol particles used do not affect the crystallization temperature starting point (T_{cm}) of the material, and its values remain 118 ± 0.5°C.

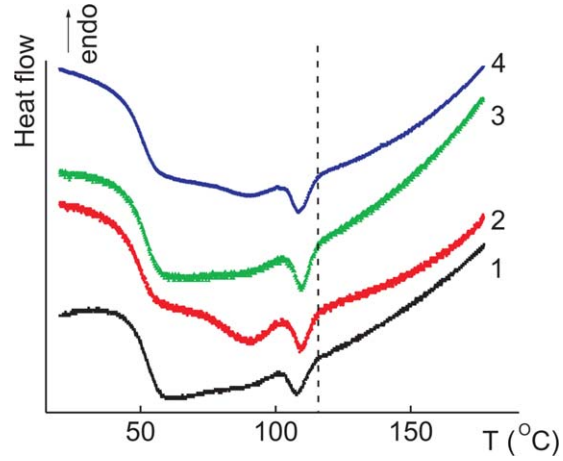

Figure 8. Hot-melt crystallization thermograms of PLA (1) and its composites containing 10 wt % "large" silicasol particles with (methoxyacetyl)oxy (1, $R = 1.7$ nm), acetoxy (2, $R = 1.5$ nm), and γ-hydroxypropylic surface groups (3, $R = 1.7$ nm). The composite crystallization starting point is marked by a dashed line. [Color figure can be viewed in the online issue, which is available at wileyonlinelibrary.com.]

However, in the presence of nanoparticles, the process of matrix polymer crystallization differs from the primary PLA crystallization.

In the cooling process of unfilled PLA, we can observe only one peak on the thermogram, the maximum temperature of which is equal to 108°C. On the thermograms of composite samples, one more peak (beyond the above-mentioned peak) at 87°C is observed. The area of the first high-temperature peak varies only slightly with the concentration of polymer filling, but the area of the second low-temperature crystallization peak (as is observed from the thermograms in Figure 7) depends on the particle concentration, their radii and the chemical structure of their surface layer. An increase or decrease in this low-temperature peak stipulates a relevant change in the specific heat of the matrix polymer composite crystallization (ΔH_{cm}).

In Table V, the ΔH_{cm} values of the systems analysed are represented. If the represented values are compared, it can be stated that the greatest differences in the matrix polymer crystallization temperatures are observed for particles with radii of 0.7 nm. Thus, the ΔH_{cm} value at $C_f = 10$ wt % for the composite with (methoxyacetyl)oxy derivatives of silicasol is 30 times that of the ΔH_{cm} value of unfilled polymer and 10 times more than the ΔH_{cm} value of the system with the same concentration but with larger sized particles. It follows that the use of hybrid silicasol particles with radii of 0.7 nm makes it possible to eliminate one of the PLA drawbacks, the low rate of its melt crystallization.

Additional research is needed to determine the reason for the second low-temperature matrix polymer crystallization peak in the presence of modified silicasol particles and, as a consequence, the relationship between the heat and rate of the crystallization of filled PLA. It is fair to assume that the hybrid nanoparticles, mainly with radii of 0.7 nm, act as secondary nucleating agents for PLA crystallization, and thus, systematizing to some extent, the macromolecular circuit ordering that increases the rate of this process.[31] Hence, the crystalline grain morphology is possibly changing.

CONCLUSIONS

PAL- and hybrid silicasol nanoparticle-based composites were obtained by extrusive blending. The results show that the hybrid particles with 0.7 nm radii act as both plasticizers and secondary nucleating agents for the matrix polymer crystallization. In the studied range of nanoparticle concentration ($C_f \leq 20$ wt %), the maximum decrease in the glass transition temperature reaches 12.8°C, for the cold crystallization temperature up to 22°C. The most significant changes in the specific heat of the matrix polymer composite crystallization are observed while filling PLA with (methoxyacetyl)oxy derivatives of molecular silicasol with 0.7 nm particle radii. As $C_f = 10$ wt %, the ΔH_{cm} value is 30 times higher than that of the unfilled polymer.

The melting points of the composites as well as their crystallization temperature starting points are the least sensitive characteristic of the material in relation to particle content, size, and type of grafted surface groups.

Introducing the particles of 1.5 or 1.7 nm radii into PLA does not influence the composite glass transition temperatures notwithstanding of their size, the nature of surface groups and matrix compatibility level. The cold crystallization temperature decreases for 13°C only in the case of (methoxyacetyl)oxy derivatives.

To sum up the reported results, it is possible to draw the following conclusion. Nanocomposites can be obtained by means of extrusive blending without any additional mixture disaggregation if hybrid particles, the organic shells of which are highly compatible with the matrix polymer, are used. The chemical structure of the surface layer of the nanoparticles as well as their sizes and concentration are the important factors in managing the structure and properties of the polymer nanocomposite. Variations in these filler parameters make it possible to conduct a controlled change of the characteristics of the composites, particularly to eliminate one of the drawbacks of PLA, the low speed of its crystallization.

CONTRIBUTION OF AUTHORS

All the listed authors significantly contribute to the article. Andrey Zhiltsov, Olga Gorbatsevitch, Valentina Kazakova synthesized and characterized molecular silicasols with external layers of different chemical nature. Oleg Gritsenko was in charge of composite preparation by means of extrusion blending. Natalia Bessonova was responsible for calorimetric analysis of PLA and composites based on it. Andrey Askadskii evaluated the compatibility between PLA matrix and molecular silica nanoparticles. Olga A. Serenko selected nanoparticles samples, commented on composite materials properties as well as summarized the experimental data. Aziz M. Muzafarov took an active part in the result discussion and helped to gain a better insight into the problem.

ACKNOWLEDGMENTS

This study was supported by the Russian Foundation for Basic Research (project no. 12-03-00922).

REFERENCES

1. Rasal, R. M.; Janorkar, A. V.; Hirt, D. E. *Prog. Polym. Sci.* **2010**, *35*, 338.
2. Auras, R.; Harte, B.; Selke, S. *Macromol. Biosci.* **2004**, *4*, 835.
3. Lim, L. T.; Auras, R.; Rubino, M. *Prog. Polym. Sci.* **2008**, *33*, 820.
4. Wen, X.; Lin, Y.; Han, C.; Zhang, K.; Ran, X.; Li, Y.; Dong, L. *J. Appl. Polym. Sci.* **2009**, *114*, 3379.
5. Södergard, A.; Stolt, M. *Prog. Polym. Sci.* **2002**, *27*, 1123.
6. Raquez, J. M.; Habibi, Y.; Murariu, M.; Dubois, P. *Prog. Polym. Sci.* **2013**, *38*, 1504.
7. Arora, A.; Padua, G. W. *J. Food Sci.* **2010**, *75*, 43.
8. Henriette, M. C.; de, A. *Food Res. Int.* **2009**, *42*, 1240.
9. Ray, S. S.; Okamoto, M. *Macromol. Rapid Comm.* **2003**, *24*, 815.
10. Mai, Y. W.; Yu, Z. Z. In Polymer Nanocomposites. Woodhead Publishing Ltd.: Cambridge, **2006**.
11. Kontou, E.; Niaounakis, M.; Georgiopoulos, P. *J. Appl. Polym. Sci.* **2011**, *122*, 1519.
12. Njuguna, J.; Pielichowski, K.; Desai, S. *Polym. Adv. Technol.* **2008**, *19*, 947.
13. Qiao, R.; Deng, H.; Putz, K. W.; Brinson, L. C. *J. Polym. Sci. Part B: Polym. Phys.* **2011**, *49*, 740.
14. Aso, O.; Eguiazábal, J. I.; Nazábal, J. *Compos. Sci. Technol.* **2007**, *67*, 2854.
15. Murariu, M.; Doumbia, A.; Bonnaud, L.; Dechief, A. L.; Paint, Y.; Ferreira, M.; Campagne, C.; Devaux, E.; Dubois, P. *Biomacromolecules* **2011**, *12*, 1762.
16. Zhu, A.; Diao, H.; Rong, Q.; Cai, A. *J. Appl. Polym. Sci.* **2010**, *116*, 2866.
17. Chaudhuri, R. G.; Paria, S. *Chem. Rev.* **2012**, *112*, 2373.
18. Yan, S.; Yin, J.; Yang, Y.; Dai, Z.; Ma, J.; Chen, X. *Polymer* **2007**, *48*, 1688.
19. Dintcheva, N. Tz.; Morici, E.; Arrigo, R.; La Mantia, F. P.; Malatesta, V.; Schwab, J. J. *Express. Polym. Lett.* **2012**, *6*, 561.
20. Paul, D. R.; Newman, S. In Polymer Blends; V. 1. Academic Press, Inc.: New York, **1978**.
21. Kazakova, V. V.; Zhiltsov, A. S.; Gorbatsevitch, O. B.; Meshkov, I. B.; Pletneva, M. V.; Demchenko, N. V.; Cherkaev, G. V.; Muzafarov, A. M. *J. Inorg. Organomet. Polym. Mater.* **2012**, *22*, 564.
22. Grubisic, Z.; Rempp, R.; Benoir, H. *J. Polym. Sci. Part B: Polym. Phys.* **1967**, *5*, 753.

23. Askadskii, A. A. In Physical Properties of Polymers: Prediction and Control. Gordon and Breach Publishers: Amsterdam, **1996**.
24. Askadskii, A. A. In Computational Materials Science of Polymers. Cambridge International Science Publishing: Cambridge, **2003**.
25. Rana, D.; Mandal, B. M.; Bhattacharyya, S. N. *Macromolecules* **1996**, *29*, 1579.
26. Rana, D.; Kim, H. L.; Kwag, H.; Rhee, J.; Cho, K.; Woo, T.; Lee, B. H.; Choe, S. *J. Appl. Polym. Sci.* **2000**, *76*, 1950.
27. Rana, D.; Cho, K.; Woo, T.; Lee, B. H.; Choe, S. *J. Appl. Polym. Sci.* **1999**, *74*, 1169.
28. Rana, D.; Lee, C. H.; Cho, K.; Lee, B. H.; Choe, S. *J. Appl. Polym. Sci.* **1998**, *69*, 2441.
29. Tanahashi, M. *Materials* **2010**, *3*, 1593.
30. Roldugin, V. I.; Serenko, O. A.; Getmanova, E. V.; Karmishina, N. A.; Chvalun, S. N.; Muzafarov, A. M. *Dokl. Chem.* **2013**, *449*, 552.
31. Wunderlich, B. In Macromolecular Physics. V.2 Crystal Nucleation, Growth, Annealing. Academic Press, Inc.: New York, **1976**.